Neoplasia 58 (2024) 101069

Contents lists available at ScienceDirect

Neoplasia

journal homepage: www.elsevier.com/locate/neo

Original Research

ARID1A loss sensitizes colorectal cancer cells to floxuridine

Cheng Xiang [a,b,1], Zhen Wang [a,1], Yingnan Yu [a,1], Zelong Han [a], Jingyi Lu [a], Lei Pan [a], Xu Zhang [a], Zihuan Wang [a], Yilin He [a], Kejin Wang [a], Wenxuan Peng [a], Side Liu [a,*], Yijiang Song [c,*], Changjie Wu [a,*]

[a] Guangdong Provincial key laboratory of Gastroenterology, Department of Gastroenterology, Nanfang hospital, Southern Medical University, Guangzhou, 510515, China
[b] Comprehensive Medical Treatment Ward, Nanfang Hospital, Southern Medical University, Guangzhou, 510515, China
[c] Department of Laboratory Medicine, Nanfang Hospital, Southern Medical University, Guangzhou, 510515, China

ARTICLE INFO

Keywords:
Synthetic lethality
ARID1A
floxuridine
5-Fu
Targeted therapies

ABSTRACT

The loss-of-function mutation of AT-rich interactive domain 1A (ARID1A) frequently occurs in various types of cancer, making it a promising therapeutic target. In the present study, we performed a screening of an FDA-approved drug library in ARID1A isogenic colorectal cancer (CRC) cells and discovered that ARID1A loss sensitizes CRC cells to floxuridine (FUDR), an antineoplastic agent used for treating hepatic metastases from CRC, both *in vivo* and *in vitro*. As a pyrimidine analogue, FUDR induces DNA damage by inhibiting thymidylate synthase (TS) activity. ARID1A, as a regulator of DNA damage repair, when lost, exacerbates FUDR-induced DNA damage, leading to increased cell apoptosis. Specifically, ARID1A deficiency impairs DNA damage repair by downregulating Chk2 phosphorylation, thereby sensitizing cancer cells to FUDR. Notably, we found that FUDR exhibited increased sensitivity in ARID1A-deficient cells compared to 5-fluorouracil (5-FU), a commonly used anticancer drug for CRC. This suggests that FUDR is superior to 5-FU in treating ARID1A-deficient CRC. In conclusion, ARID1A loss significantly heightens sensitivity to FUDR by promoting FUDR-induced DNA damage in CRC. These findings offer a novel therapeutic approach for the treatment of CRC characterized by ARID1A loss-of-function mutations.

Introduction

Colorectal cancer (CRC) is one of the most frequently observed malignancies and the second leading cause of cancer-related deaths worldwide [1-3]. Metastasis is the major cause of death in patients with CRC and the most common site of metastasis is the liver [4-6]. It is estimated that up to 60 % of CRC patients develop distant metastasis within five years of diagnosis [7]. Despite advancements in treatment, including cytotoxic chemotherapy, targeted agents, and immune checkpoint inhibitors, the five-year survival rate for metastatic CRC remains dismally low at around 20 % [8,9]. Thus, novel targeted therapies are urgently needed for CRC, particularly for late-stage CRC.

ARID1A (AT-rich interactive domain 1A) encodes a crucial subunit of the SWI/SNF chromatin remodeling complex and has been identified as one of the most frequently mutated tumor suppressor genes across various cancer types [10-12]. In CRC, approximately 10 % of patients harbor mutations in ARID1A [13]. Moreover, ARID1A expression is strongly associated with distant metastasis, and the frequency of ARID1A loss increases with advancing tumor-node-metastasis (TNM) stages [14]. Specifically, ARID1A loss has been observed in 7.4 % of stage I samples, 24.1 % of stage II samples, 22.2 % of stage III samples, and a significant 46.3 % of stage IV samples [14]. These data suggest that ARID1A has a higher rate of loss-of-function mutations in metastasis CRC patients, making it a potential therapeutic target for anticancer drug development.

Synthetic lethality, a genetic interaction where the deficiency of a single gene does not affect cell viability but the combination of deficiencies in two genes leads to cell death, has been widely exploited in cancer therapy [15,16]. This concept is particularly relevant because many cancers harbor loss-of-function mutations in tumor suppressor genes that are challenging to target directly. By identifying synthetic lethal partners of these mutated genes, it is possible to develop targeted therapies that selectively kill cancer cells while sparing normal cells [17,18]. Based on the concept of synthetic lethality, we initiated a

* Corresponding authors.
E-mail addresses: sideliu@smu.edu.cn (S. Liu), songyj@smu.edu.cn (Y. Song), backkom8788@smu.edu.cn (C. Wu).
[1] These authors contributed equally to this work.

https://doi.org/10.1016/j.neo.2024.101069
Received 6 August 2024; Received in revised form 28 September 2024; Accepted 8 October 2024

systematic screening using an isogenic CRC cell pair with and without ARID1A expression, along with an FDA-approved drug library. Our screening identified floxuridine (FUDR) as a drug that exhibits increased antitumor activity in ARID1A-deficient CRC cells.

FUDR, a pyrimidine analogue, is used as an antineoplastic agent for treating hepatic metastases from colon cancer [19-21]. It exerts its cytotoxic effects by inhibiting thymidylate synthase (TS), an enzyme necessary for DNA synthesis, thereby inducing DNA damage and inhibiting cell proliferation [22]. ARID1A plays a crucial role in facilitating DNA damage repair. Loss of ARID1A results in DNA repair defects, making cells more susceptible to DNA-damaging agents [23-25]. Therefore, ARID1A loss exacerbates FUDR-induced DNA damage, leading to increased cell apoptosis. Interestingly, our study revealed that ARID1A-deficient CRC cells are more sensitive to FUDR compared to 5-fluorouracil (5-FU), a commonly used chemotherapeutic agent in CRC [26]. This finding suggests that FUDR could be a superior therapeutic option for treating ARID1A-deficient CRC.

Materials and methods

Cell culture and reagents

CRC cell lines, HCT116 and RKO were obtained from American Type Culture Collection (ATCC, Manassas, VA), which have been authenticated by the provider. HCT116 was cultured in RPMI-1640 media supplemented with 10 % fetal bovine serum (FBS) and 1 % penicillin/streptomycin. RKO was cultured in Dulbecco's modified Eagle's medium supplemented with 10 % FBS and 1 % penicillin/streptomycin. Cells were maintained in a humidified incubator adjusted with 5 % CO_2 at 37 °C.

FDA-approved drug library screening and cell viability measurement

FDA-approved drug library containing 425 drugs was purchased from TargetMol (Shanghai, China). Each compound was arrayed in 384-well plates at the same 20μM-dose. HCT116 *ARID1A* WT or *ARID1A* KO cells were seeded at 2000 cells per well in the 384-well plates containing working dilution of the compound library and incubated for 72 h at 37 °C CO_2 incubator. All the liquid handling was done with Liquidator-12 multi-well pipettor (Gilson PIPETMAN® L, France). For cell viability measurement, cells were incubated with Alamar Blue solution (Sigma-Aldrich, St. Louis, MO) at 10 % for 2 h and the fluorescence signal (ex560/em590) at the bottom of the plate was measured with SpectraMax-M4 (Molecular Devices, Sunnyvale, CA). The screening was done in duplicated and the average fluorescence intensity from the two screenings were used to identify synthetic lethality hits. Z score was calculated according to the following equation: Z score = (Log (2, KO/WT)-Mean)/STDEV. Compounds with Z score < -2 were selected as candidates.

Immunoblot and antibodies

Whole-cell protein extracts were prepared with ice-cold RIPA buffer (25 mM Tris-HCl pH 7.6, 150 mM NaCl, 1 % NP-40, 1 % sodium deoxycholate, 0.1 % sodium dodecyl sulfate (SDS)) with Complete Protease Inhibitor Cocktail (Roche Life Sciences, Indianapolis, IN). Each aliquot of protein sample was run on a SDS-polyacrylamide gel electrophoresis and transferred onto a PVDF membrane for immunoblotting with primary antibodies, including ARID1A (Cell Signaling Technology, #12354s, 1:1000 dilution), β-actin (Cell Signaling Technology, #3700s, 1:2000 dilution), cleaved PARP (Cell Signaling Technology, #5625s, 1:1000 dilution), cleaved caspase 3 (Cell Signaling Technology, #9661s, 1:1000 dilution), GAPDH (Fdbio Technology, FD0063, 1:1000 dilution), p-H2A.X (Cell Signaling Technology, #9718T, 1:1000 dilution), p-Chk1 (Cell Signaling Technology, #2348T, 1:1000 dilution), p-Chk2 (Cell Signaling Technology, #2197T, 1:1000 dilution), p-ATR (Cell Signaling Technology, #2853T, 1:1000 dilution) and p-ATM (Cell Signaling Technology, #5883T, 1:1000 dilution) antibodies, followed by horseradish peroxidase-conjugated secondary antibodies.

Organoid culture

Crypts were isolated as described previously [27,28]. Briefly, human normal intestinal fragments were washed with cold DPBS, then incubated in 5 mM EDTA with gentle shaking at 4 °C for 30–40 min. The isolated healthy crypts were counted and embedded in Matrigel (Corning, #356237) and cultured in IntestiCult™ Organoid Growth Medium (StemCell Technology, #06010) or Human Intestinal Stem Cell medium (HISC, comprised with advanced DMEM/F12 medium, GlutaMAX, HEPES, penicillin, streptomycin, N2, B27, N-acetylcysteine, noggin, R-spondin 1, EGF, WNT3a, A83–01, SB202190, FGF10, nicotinamide, gastrin, Prostaglandin E2, and Y27632). The medium was changed every 2 or 3 days.

Cell apoptosis assays

For apoptosis analysis, FITC–Annexin V Apoptosis Detection Kit with PI (MULTISCIENCES, Hangzhou, China) was used. Briefly, cells were washed with ice-cold PBS and re-suspended with Annexin V staining buffer. The cells were then stained with fluorescein isothiocyanate (FITC)–Annxin V and PI at room temperature for 15 min and then analyzed immediately with a CytoFLEX Flow Cytometer (Beckman Coulter Life Sciences, CA).

Comet assay

DNA damage was determined by an alkaline Comet assay. Briefly, alkaline comet assay was detected by the manufacturer's protocol of the Reagent Kit for Single Cell Gel Electrophoresis Assay (KeyGEN BioTECH, Nanjing, China). First of all, lysis cells with pre-chilled lysis buffer. After lysis, gels were transferred to an electrophoresis chamber filled with alkaline unwinding buffer (1 mmol/L EDTA, 300 mmol/L NaOH) for 20–60 min at room temperature. Electrophoresis was conducted with the same buffer in 25 V for 30 min. After adding buffer solution (0.4 mmol/L Tris-HCl) for neutralization, add PI dye solution to stain for 10 min in the dark. The experimental results were collected using a fluorescence inverted microscope (Olympus IX73). The results of the comet assay were analyzed using Comet Assay Software Project. Briefly, 50 cells were randomly selected in each sample for measurement, and the percentage of tail DNA content to head DNA content (Tail DNA%) was calculated.

TUNEL staining

The TUNEL assay was carried out using a One-Step TUNEL Apoptosis Assay Kit (Beyotime, Shanghai, China). Briefly, cells were seeded on confocal laser culture dishes. All dishes were washed by PBS, and fixed with 4 % paraformaldehyde solution for 20 min. Then washed by PBS and added PBS containing 0.25 %Triton X-100 for 15 min in the ice bath. And the labelling reaction was performed using a labelling solution containing terminal deoxynucleotidyl transferase, its buffer, and fluorescein dUTP at 37 °C for 60 min in a humidity chamber. Following incubation, excess labelling solution is washed off with PBS and the cell smears are mounted on coverslips with Anti-fade Fluorescence Mounting Medium, and the nuclei were stained with DAPI. Images were captured using a Laser Scanning Microscope (Olympus FV1200, Tokyo, Japan).

Tumor xenograft mouse model

All animal procedures were approved by the Animal Research Ethics Committee of Nanfang Hospital and were carried out according to

ARRIVE guidelines. Eight-week-old, female BALB/c nude mice were implanted with *ARID1A*-WT (left flank) and *ARID1A*-KO (right flank) HCT116 cells suspended in Matrigel. When both tumors were palpable, mice were randomized into 3 groups ($n = 5$ mice per group) of equal tumor volume for treatment with vehicle and FUDR, but the researchers were not blinded to the groups when performing the experiments. Mice were intravenously injected with vehicle (sterile saline containing 5 % dimethyl sulfoxide, 5 % tween-80, and 5 % polyethylene glycol-400) or FUDR (5 and 10 mg/kg, 100 μL) via tail vein every three days for 18 days. The tumor size was periodically measured with a Vernier caliper and the tumor volume was calculated based on the modified ellipsoid formula (long axis × short axis^2 × π/6). At the end of experiments, mice were sacrificed and the tumors were harvested for weighing and further analyses. Mice body weights were measured regularly during the drug injection period to assess potential drug toxicity.

Statistical analysis

All data were expressed as the mean ± standard deviation (s.d.). Statistical significance of differences between control and test groups was determined by Student's *t* test or one-sample *t* test using Graphpad Prism 8 (GraphPad Software, La Jolla, CA). Statistical analysis of differences between two dose–response curves was determined by analysis of variance using Graphpad Prism 8. All statistical tests were two tailed. *P* values < 0.05 were considered significant.

Results

FDA approved drug library screening identifies FUDR as a synthetic lethal partner of ARID1A

As a tumor suppressor gene, *ARID1A* is mutated in approximately 10 % of CRC patients. To verify this result, we analyzed ARID1A mutation status of 753 colorectal cancer samples using the cBioPortal platform (Supplementary Fig. 1). Our analysis revealed an overall ARID1A mutation rate of approximately 12 % (86 out of 753 samples). Among these mutations, truncating mutations were the most frequent (65 out of 86), followed by missense mutations (19 out of 86), with deep mutations and splice mutations each occurring once (1 out of 86). In summary, 78 % of the mutations were inactivating, while 22 % were of unknown significance. This result indicated that ARID1A could be a therapeutic target for cancer treatment.

To identify potential ARID1A synthetic lethal drugs, we used ARID1A-isogenic HCT116 CRC pairs generated by CRISPR / Cas9 system [29]. The ARID1A status was confirmed by western blot (Fig. 1A). Then we performed a screening of a drug library which contains 422 FDA approved drugs. The screening was conducted at a dose of 20 μM in 384-well plates, and cell viabilities were measured using Alamar blue assay (Fig. 1B). After two rounds of screening, we identified three candidate drugs with Z scores less than -2: floxuridine (an inhibitor of DNA synthesis), Nilutamide (a nonsteroidal anti-androgen), and LDK378 (an ALK inhibitor) (Fig. 1C). To further validate our screening results, we conducted killing curves in two *ARID1A* knockout (*ARID1A*-KO) clones with the candidate compounds. It was evident that only floxuridine (FUDR) exhibited a higher inhibition efficiency in the two *ARID1A*-KO clones compared to *ARID1A*-WT cells (Fig. 1D-F). Therefore, these results suggest that FUDR has a significant synthetic lethal effect with ARID1A loss in CRC cells.

FUDR represses the growth of ARID1A-deficient CRC cells

To further investigate the synthetic lethal effect of FUDR and ARID1A, cell morphology experiments were conducted in two *ARID1A* knockout clones. The results showed that FUDR significantly repressed cell viability of *ARID1A*-KO cells compared with *ARID1A*-WT HCT116 cells (Fig. 2A-B). To further validate synthetic lethal effect of FUDR, we established another isogenic cell pair derived from RKO CRC cell line, which has a frameshift mutation in ARID1A [25,29], via lentivirus transfection. The ARID1A expression level was detected with western

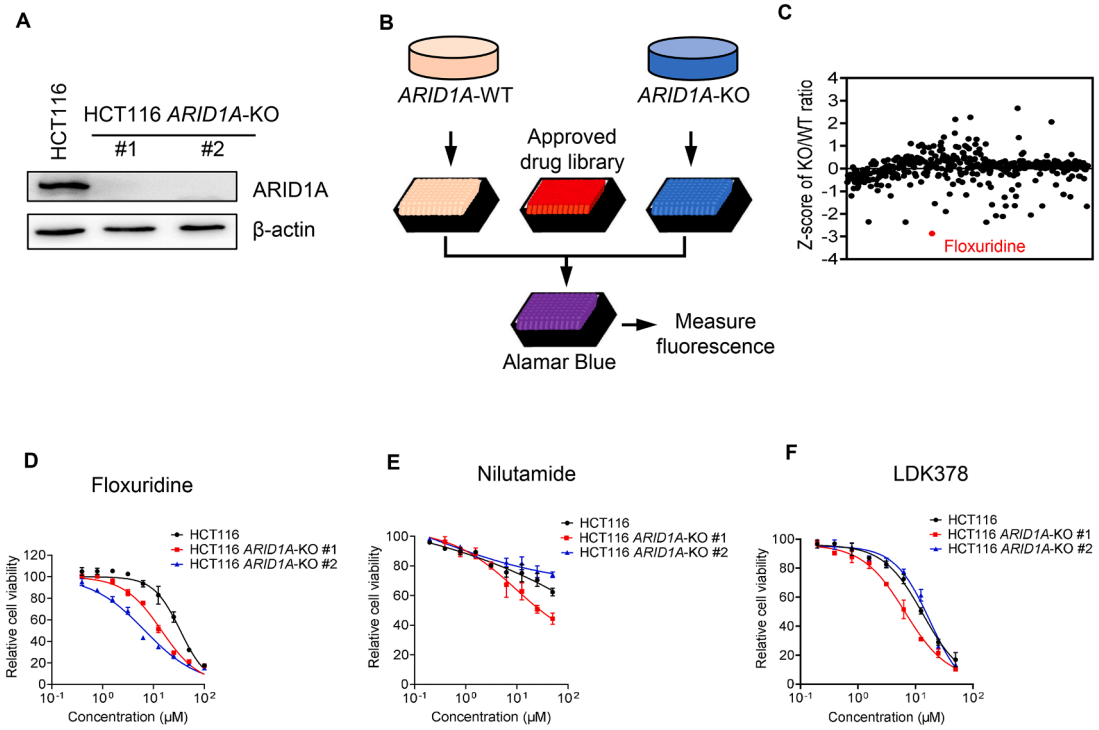

Fig. 1. Screening of FDA approved drug library for synthetic lethality in HCT116 isogenic cells. (A) Western blotting analysis status was confirmed in two HCT116 *ARID1A*-KO cells. (B) Schematic diagram of the FDA-approved drug library screening. (C) The Z-score of screening. (D-E) Dose–response curves of HCT116 *ARID1A*-WT and two *ARID1A*-KO cells treated with FUDR,Nilutamide and LDK378 for 72 h are shown.

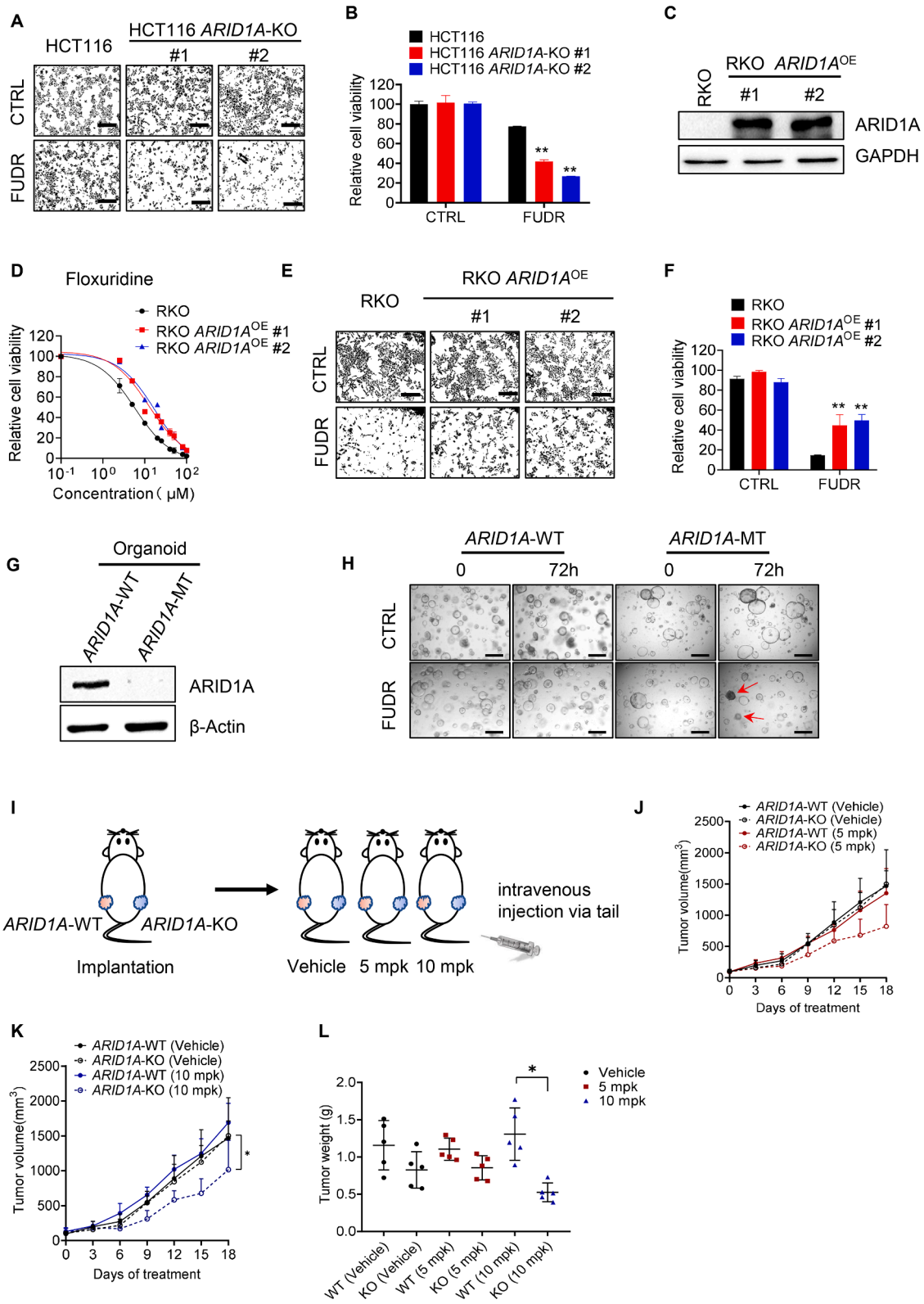

Fig. 2. FUDR represses growth of ARID1A-deficient CRC cells *in vitro* and *in vivo*. (A) Cell morphology of synthetic lethal in HCT116 *ARID1A*-KO cells by FUDR. Images were taken with Olympus IX73. Scale bars, 300 μm. (B) Cell density was measured with Image J software as a surrogate for cell viabilities. Error bars represent s.d. **P < 0.01, Student's t test. (C) Immunoblot analysis showing overexpression of ARID1A. (D) Dose–response curves of parental RKO and ARID1A overexpressing (*ARID1A*^{OE}) RKO clones with FUDR. Error bars represent s.d. (E) Cell morphology of synthetic lethal in HCT116 *ARID1A*-KO cells by FUDR. Images were taken with Olympus IX73. Scale bars, 300 μm. (F) Cell density was measured with Image J software as a surrogate for cell viabilities. Error bars represent s.d. **P < 0.01, Student's t test. (G) Western Blot analysis of ARID1A expression in two CRC organoids. (H) Micrographs of organoids treated with or without 100 μM FUDR for 3 days. Representative organoids were marked with red arrow. Scale bar, 500 μm. (I) Schematic diagram shows tumor xenograft experiments with HCT116 ARID1A isogenic cell pair. (J-K) The size of tumor xenografts was measured every 3 days and tumor growth curve was displayed. Data are presented as the mean ± SEM. (L) Wet weight of the dissected tumor samples was measured.

blot (Fig. 2C). Killing curve and cell morphology experiments were produced with two RKO ARID1A overexpression (*ARID1A*^{OE}) clones. Consistent with the HCT116 isogenic cell pair, FUDR treatment results in synthetic lethality with ARID1A deficiency was observed (Fig. 2D-F). These results suggest that FUDR treatment results in synthetic lethality with ARID1A loss *in vitro*. This result was further validated in HCT116 and RKO cell lines. RKO cells, which lack ARID1A expression, were significantly more sensitive compared to HCT116 cells that express ARID1A (Supplementary Fig. 2). These findings strengthen the reliability of our conclusions.

To further investigate the role of ARID1A in determining FUDR sensitivity in preclinical models, we established two patient-derived CRC organoids—one with ARID1A expression (*ARID1A*-WT) and one without (*ARID1A*-MT). Western blot analysis confirmed that the *ARID1A*-WT organoid exhibited significantly higher ARID1A expression compared to the *ARID1A*-MT organoid (Fig. 2G). To assess the response to FUDR treatment, we exposed both organoids to FUDR. Interestingly, the *ARID1A*-MT organoid demonstrated a greater reduction in both organoid number and size compared to the *ARID1A*-WT organoid, indicating a higher sensitivity to FUDR (Fig. 2H). These findings suggest that ARID1A expression levels play a crucial role in determining the FUDR sensitivity of patient-derived CRC organoids.

Furthermore, we evaluated the antigrowth effect of FUDR in a tumor xenograft mouse model. Mice bearing ARID1A isogenic tumors in flanks were given FUDR or Vehicle via intravenous injection every three days, body weights and tumor volumes were measured periodically (Fig. 2I). We found FUDR treatment inhibited tumor growth without ARID1A expression especially at the concentration of 10 mpk, which was in line with our *in vitro* fundings (Fig. 2J-L). FUDR injection every three days did not appear to cause toxicity in mice as assessed by body weight changes (Supplementary Fig. 3). In summary, these results demonstrate that FUDR treatment induces synthetic lethality in ARID1A-deficient CRC cells, both *in vitro* and *in vivo*.

FUDR induces apoptosis in ARID1A-deficient CRC cells

As an antineoplastic agent, FUDR generates F-dUMP and FUMP, which covalently bind to the active center of thymidylate synthase. This binding inhibits the enzyme's activity, leading to a deficiency in deoxynucleotides and obstruction of DNA synthesis, ultimately inducing cell apoptosis. Therefore, we analyzed the phenotype of CRC cells following FUDR treatment. After treatment with 10 μM FUDR for 48 hours, HCT116 *ARID1A*-WT and *ARID1A*-KO cells were collected and subjected to cell apoptosis analysis using flow cytometry. The results showed a significantly increase of cell apoptosis in *ARID1A*-KO cells than *ARID1A*-WT cells (Fig. 3A-B). Consistent with the results in HCT116 cells, FUDR treatment in RKO isogenic cells selectively increased apoptosis in ARID1A-deficient cells (Fig. 3C-D). Furthermore, immunoblot analysis of cleaved PARP and cleaved caspase-3, indicators of cell apoptosis, revealed significantly higher levels of apoptosis in *ARID1A*-KO cells following FUDR treatment (Fig. 3E-F). These results suggest that ARID1A loss sensitizes CRC cells to FUDR-induced cell apoptosis.

ARID1A-deficient CRC cells are more sensitive to FUDR than to 5-FU

Fluorouracil (5-FU) is an important anticancer drug and has been used for more than 60 years in the treatment of CRC. Both FUDR and 5-FU are pyrimidine analogues which can inhibit the proliferation of cancer cells by interfering with DNA synthesis and RNA function. In addition to inhibiting thymidylate synthase activity, FUDR can convert to 5-FU to play anticancer function. Therefore, in order to clarify the difference between FUDR and 5-FU in the treatment of ARID1A-deficient cells, we compared their antitumor effect in HCT116 and RKO ARID1A-isogenic cells. Interestingly, the results showed that both FUDR and 5-FU sensitivity increased in *ARID1A* knockout HCT116 cells, with FUDR demonstrating higher sensitivity than 5-FU in ARID1A-deficient cells at the same concentration (Fig. 4A). These results were further confirmed with two HCT116 *ARID1A*-KO clones and RKO ARID1A-isogenic cells (Fig. 4B-C). Following FUDR and 5-FU treatment, the percentage of cell apoptosis cells showed a significant increase, especially with FUDR treatment (Fig. 4D-E). These results are consistent with those of the immunoblot analysis. Cell apoptosis markers (Cleaved PARP and Cleaved caspase 3) were specifically increased in ARID1A-deficient cells and FUDR has a higher sensitivity compared with 5-FU (Fig. 4F). Similar results were observed in RKO isogenic cells (Fig. 4G-I). Taken together, these results indicate that ARID1A deficiency sensitizes CRC cells to FUDR and 5-FU, and compared with 5-FU, ARID1A deficient cells is more vulnerable to FUDR.

ARID1A loss exacerbates FUDR-induced DNA damage

FUDR functions as a thymidylate synthase (TS) inhibitor, but the exact molecular mechanisms that mediate events downstream of TS inhibition have not been fully elucidated. TS catalyses the reductive methylation of deoxyuridine monophosphate (dUMP) to deoxythymidine monophosphate (dTMP). Therefore, TS inhibition leads to dTMP depletion and dUMP accumulation, both of which will lead to lethal DNA damage (Fig. 5A). Considering that ARID1A is involved in DNA damage repair, we hypothesized that ARID1A loss might enhance FUDR-induced DNA damage. To test this hypothesis, we first investigated the DNA damage with FUDR treatment in HCT116 and RKO ARID1A isogenic cells. Our results showed that FUDR treatment increases DNA damage as indicated by the comet and TUNEL assay in ARID1A deficient cells compared with ARID1A-WT cells (Fig. 5B-G). Meanwhile, similar as cell phenotype results, FUDR treatment induced more sever DNA damage accumulation than 5-FU treatment which give it a potential explanation why FUDR is more sensitive than 5-FU (Fig. 5D-G). To further investigated the importance of DNA damage in the synthetic lethality between ARID1A and FUDR, we checked DNA damage associated proteins with western blot, including p-ATM, p-ATR, p-Chk1, p-Chk2, and p-H2AX. According to the results, HCT116 *ARID1A*-KO cells treated with FUDR displayed elevated levels of p-Chk1 and p-H2A.X, indicating increased DNA damage response (Fig. 5H). Conversely, RKO *ARID1A*^{OE} cells showed reduced levels of these proteins, suggesting a stronger resistance to DNA damage (Fig. 5I). Finally, we compared the effects of 5-FU and FUDR on the expression level of DNA damage-related proteins in *ARID1A*-KO (Fig. 5J) and *ARID1A*^{OE} cells (Fig. 5K). FUDR induced higher level of DNA damage repair protein level in ARID1A deficient cells compared with 5-FU. These results showed that ARID1A loss enhanced FUDR induced DNA damage accumulation and contributed the observed the synthetic lethality. These results suggest that FUDR induces DNA damage by inhibiting DNA synthesis. In *ARID1A*-WT cells, this DNA damage can be repaired through the activation of the ATM checkpoint signaling pathway, which involves ARID1A. Therefore, in *ARID1A*-KO cells, the lack of functional ARID1A impairs the DNA damage repair mechanism, leading to the accumulation of DNA damage and eventually causing cell apoptosis (Fig. 5L).

Discussion

In this study, we found that ARID1A loss sensitizes CRC cells to the antineoplastic drug FUDR. The observed synthetic lethality arises from the coregulation of DNA damage accumulation. FUDR induces DNA damage by inhibiting thymidylate synthase (TS), while ARID1A plays a crucial role in DNA damage repair. The loss of ARID1A impairs the DNA damage repair capability, thereby enhancing FUDR-induced DNA damage and promoting cell apoptosis. Notably, we discovered that FUDR exhibits higher sensitivity than 5-FU in ARID1A-deficient cells. Consequently, we propose that FUDR is a promising therapeutic drug for ARID1A-deficient CRC, with superior efficacy compared to 5-FU.

ARID1A is a tumor suppressor gene whose expression loss becomes

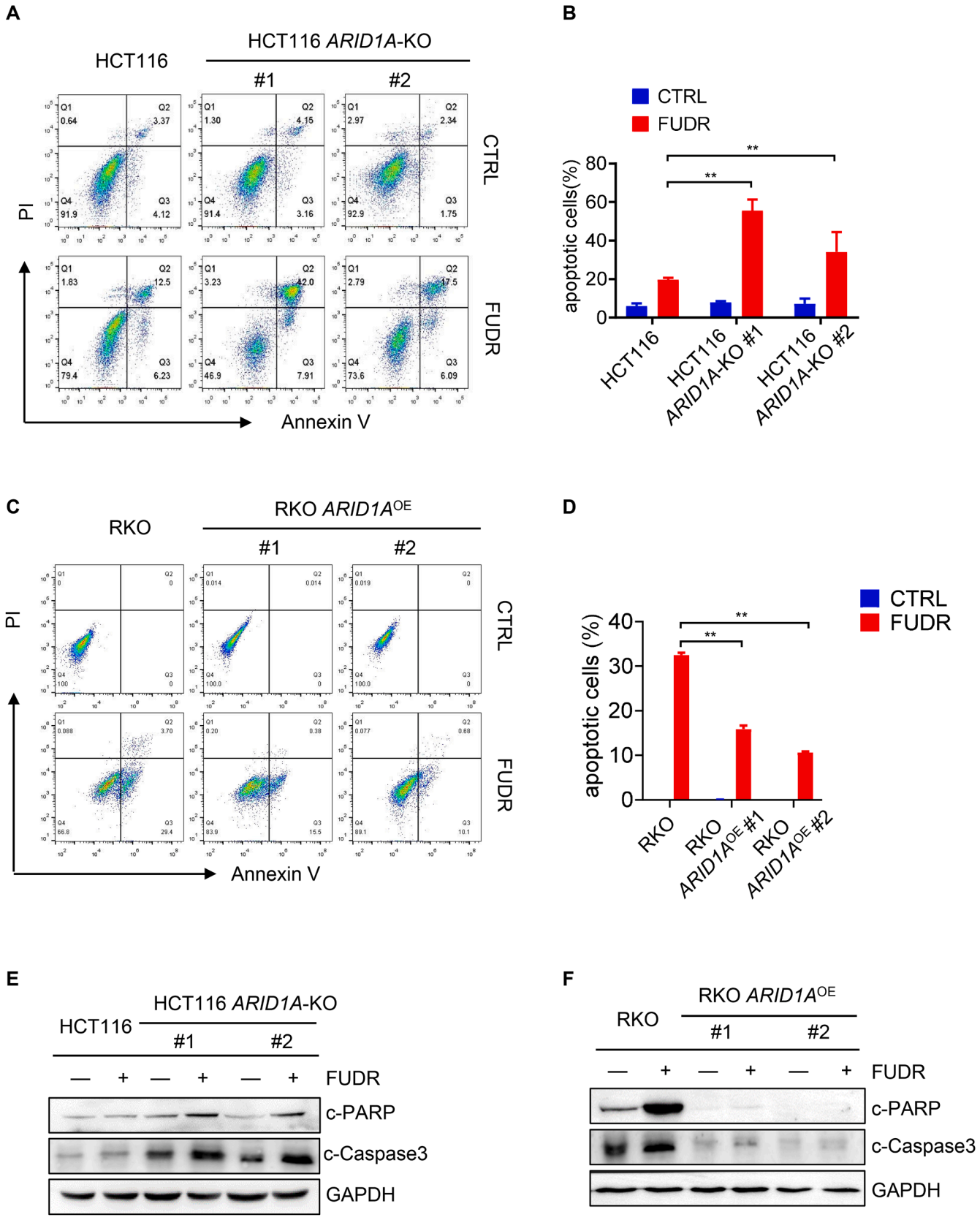

Fig. 3. ARID1A loss sensitizes cells to FUDR-induced cell apoptosis. (A) Preferential induction of apoptosis in *ARID1A*^{OE} cells by FUDR. (B) The percentage of apoptotic cells was quantitated Error bars represent s.d. *P < 0.05; **P < 0.01, Student's t test. (C) Preferential induction of apoptosis in *ARID1A*^{OE} cells by FUDR. (D) The percentage of apoptotic cells was quantitated Error bars represent s.d. *P < 0.05; **P < 0.01, Student's t test. (E-F) FUDR treatment induced Cleaved PARP and cleaved caspase-3 detection.

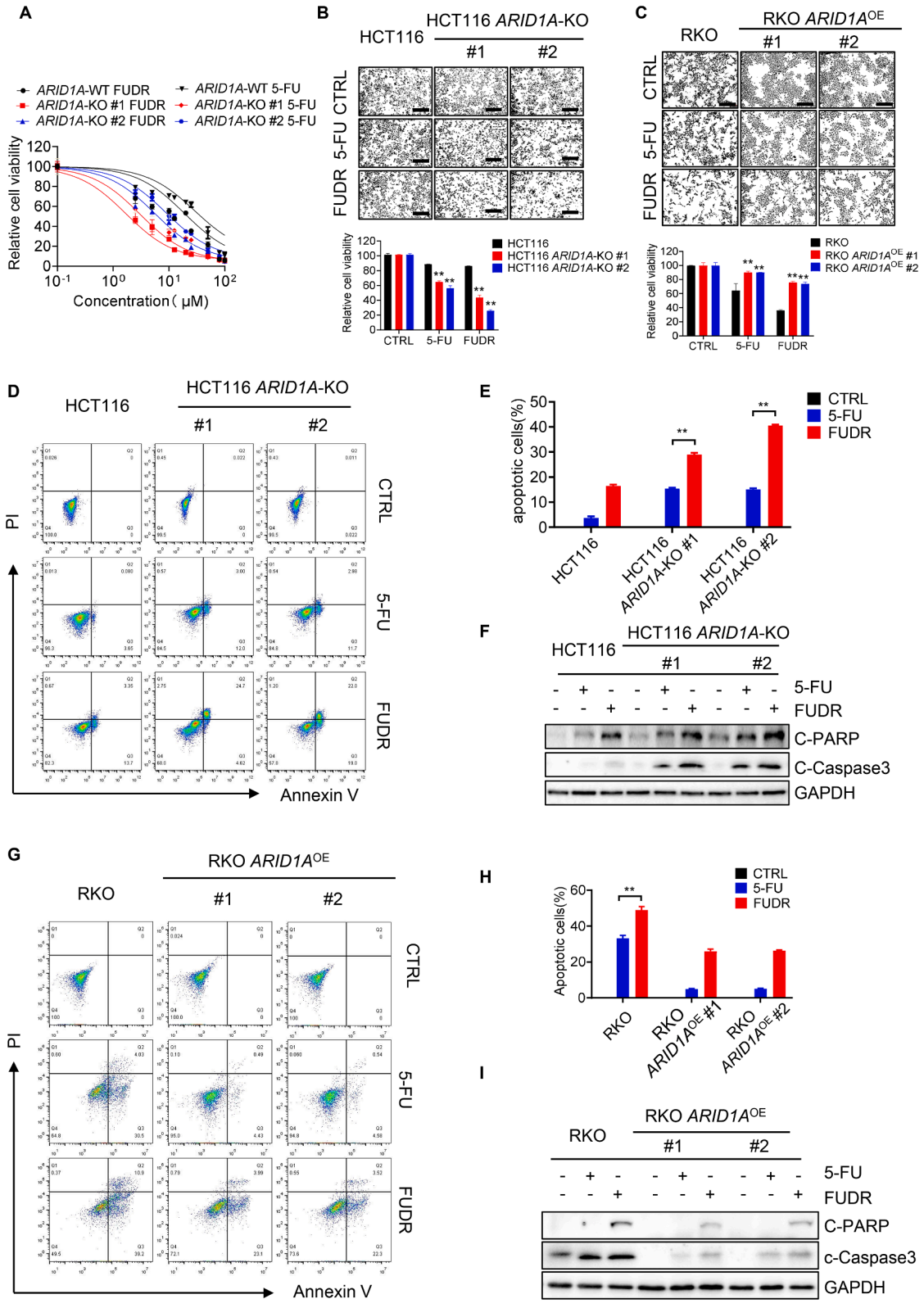

Fig. 4. ARID1A-deficient CRC cells are more sensitive to FUDR than to 5-FU. (A) Dose–response curves of parental HCT116 and *ARID1A*-KO HCT116 clones treated with 5-FU and FUDR. Error bars represent s.d. (n = 3) (B) The comparison of 5-FU and FUDR treatment of synthetic lethality in *ARID1A*-KO HCT116 cells. The cell images were taken with Olympus IX73. Scale bars, 300 μm. Cell density was measured with Image J software as a surrogate for cell viabilities. Error bars represent s. d. **P < 0.01, Student's t test. (C) The comparison of 5-FU and FUDR treatment of synthetic lethality in RKO ARID1A isogenic cells. The cell images were taken with Olympus IX73. Scale bars, 300 μm. Cell density was measured with Image J software as a surrogate for cell viability. Error bars represent s.d. **P < 0.01, Student's t test. (D) The comparison of 5-FU and FUDR treatment of preferential induction of apoptosis in *ARID1A*-KO cells. The percentage of apoptotic cells were quantitated (E). Cleaved PARP and cleaved caspase-3 level were detected in HCT116 isogenic cells (F). The comparison of 5-FU and FUDR treatment of preferential induction of apoptosis in *ARID1A*^{OE} cells (G). The percentage of apoptotic cells were quantitated (H). The comparison of 5-FU and FUDR treatment of preferential induction of Cleaved PARP and cleaved caspase-3 in RKO isogeinc cells (I).

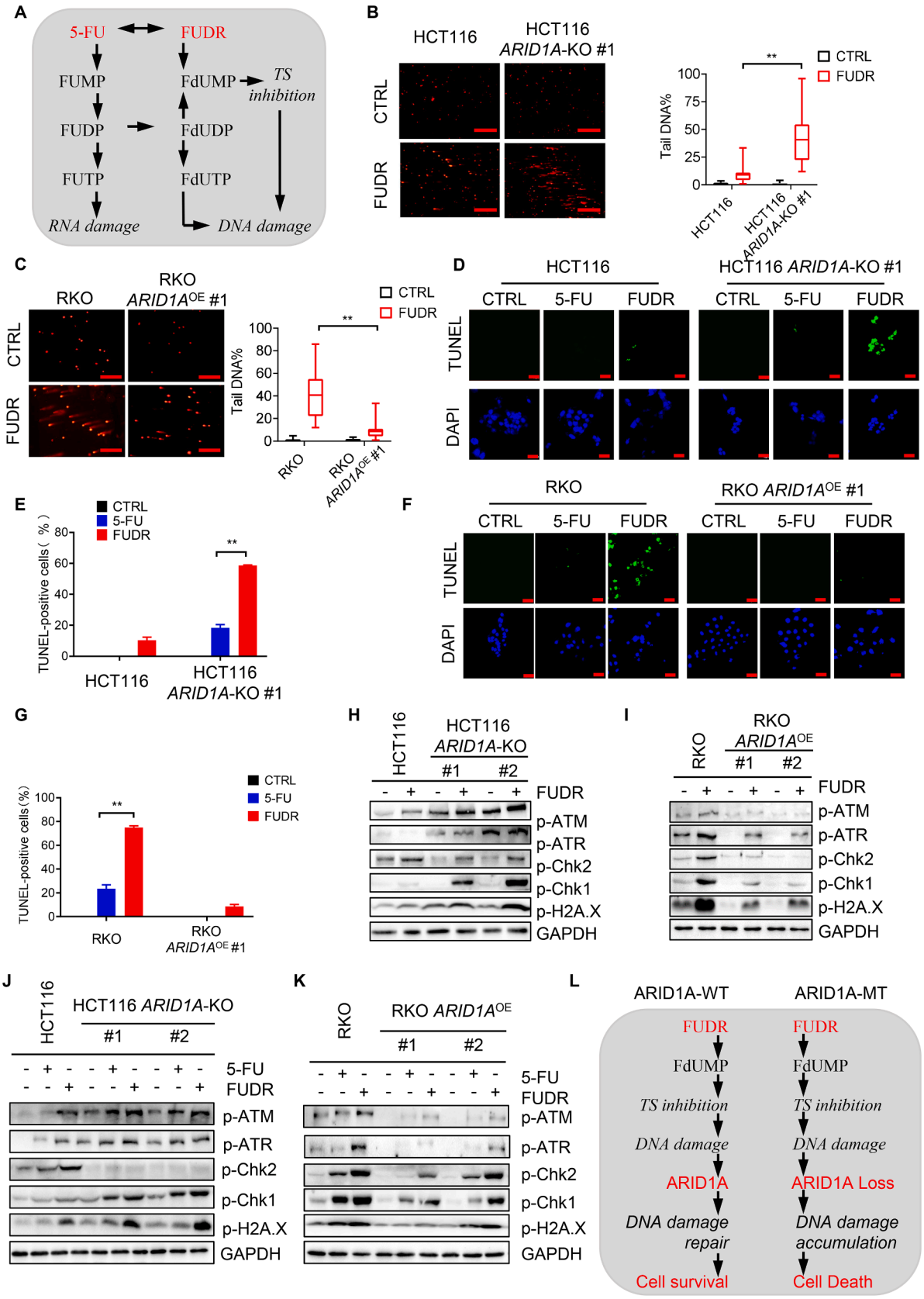

(caption on next page)

Fig. 5. ARID1A loss exacerbates FUDR-induced DNA damage. (A) Schematic diagram of FUDR and 5-FU metaboslism. (B) Representative images of HCT116 and HCT116 *ARID1A*-KO with or without FUDR treatment in the comet assay. Scale bar, 300 μm. Analyses of the percentage tail DNA in the comet assay (n=40). (C) Representative images of RKO and RKO *ARID1A*^{OE} with or without FUDR treatment in the comet assay. Scale bar, 300 μm. Analyses of the percentage tail DNA in the comet assay (n=40). (D) The comparison of 5-FU and FUDR treatment with TUNEL staining in HCT116 and HCT116 *ARID1A*-KO cells treated with 5-FU and FUDR. Images were captured using Olympus FV1200. Scale bars, 50 μm. (E) The percentage of TUNEL-positive cells was determined by counting cells in at least three fields and more than 50 cells in total. (F) The comparison of 5-FU and FUDR treatment with TUNEL staining in RKO and RKO *ARID1A*^{OE} cells treated with 5-FU and FUDR. Images were captured using Olympus FV1200. Scale bars, 50 μm. (F) The percentage of TUNEL-positive cells was determined by counting cells in at least three fields and more than 50 cells in total. (H-I) The protein level of Phospho-ATM, Phospho-ATR, Phospho-Chk1, Phospho-Chk2 and Phospho-H2A.X was detected by immunoblots. *ARID1A*-KO cells and *ARID1A*^{OE} cells were treated with 10 μM FUDR for 48 h. GAPDH was applied as an internal control. (J-K) The protein level of p-ATM, p-ATR, p-Chk1, p-Chk2 and p-H2A.X was detected by Western blot. *ARID1A*-KO cells and *ARID1A*^{OE} cells were treated with or without FUDR or 5-FU. GAPDH was applied as an internal control. (L) Working model of the synthetic lethality between ARID1A and FUDR.

more pronounced as the TNM stage of CRC advances [30]. Given that ARID1A plays a crucial role in DNA damage repair, its deficiency in advanced stages of CRC makes the cancer cells more vulnerable to DNA-damaging agents [31,32]. Our results demonstrated that FUDR, an anticancer drug, has shown promise in targeting ARID1A-deficient cells by inducing significant DNA damage, leading to increased apoptosis. Meanwhile, FUDR is more effective than 5-FU in ARID1A-deficient CRC cells, suggesting its potential as a superior therapeutic option especially for treating advanced CRC, where ARID1A loss is prevalent. By leveraging the synthetic lethality between ARID1A loss and FUDR-induced DNA damage, FUDR could offer a more targeted and effective treatment strategy for this challenging form of cancer.

Both FUDR and 5-FU are pyrimidine analogues which are used as chemotherapy drugs [22]. In cells, 5-FU is converted to three main active metabolites: fluorodeoxyuridine monophosphate (FdUMP), fluorodeoxyuridine triphosphate (FdUTP) and fluorouridine triphosphate (FUTP). The main mechanism of 5-FU activation is conversion to fluorouridine monophosphate (FUMP). FUMP is then phosphorylated to fluorouridine diphosphate (FUDP), which can be either further phosphorylated to the active metabolite fluorouridine triphosphate (FUTP), or converted to fluorodeoxyuridine diphosphate (FdUDP) by ribonucleotide reductase (RR). In turn, FdUDP can either be phosphorylated or dephosphorylated to generate the active metabolites FdUTP and FdUMP, respectively. An alternative activation pathway involves the thymidine phosphorylase catalysed conversion of 5-FU to fluorodeoxyuridine (FUDR), which is then phosphorylated by thymidine kinase (TK) to FdUMP [33]. According to our results, FUDR induces more sever DNA damage than 5-FU in ARID1A-deficient cells, which indicated that compared to metabolized to FUMP, FUDR is more toxicity to cancer cells. These findings suggest that FUDR is a more effective chemotherapeutic drug than 5-FU in ARID1A-deficient CRC cells.

In summary, our findings indicated that anticancer drug FUDR exhibits a synthetic lethal effect with ARID1A loss. ARID1A loss promotes FUDR induced DNA damages and results in cell apoptosis. ARID1A-deficient CRC cells are more sensitive to FUDR compared to 5-FU. The synthetic lethality between ARID1A and FUDR presents a novel and promising therapeutic strategy for patients with ARID1A-deficient CRC.

Funding

This study was supported by the National Natural Science Foundation of China (No. 82002553, No. 82172638, No. 12202178, China), Guangzhou Science and Technology Program key projects (No. 2023B03J1236, China) and President Foundation of Nanfang Hospital, Southern Medical University (2022B039, China).

Data availability

All data supporting this study are available from the corresponding author on reasonable request.

CRediT authorship contribution statement

Cheng Xiang: Writing – original draft, Visualization, Validation, Methodology, Funding acquisition. **Zhen Wang:** Visualization, Methodology, Data curation. **Yingnan Yu:** Visualization, Validation, Methodology, Data curation. **Zelong Han:** Data curation. **Jingyi Lu:** Data curation, Methodology. **Lei Pan:** Methodology, Investigation. **Xu Zhang:** Validation, Investigation. **Zihuan Wang:** Visualization, Methodology, Data curation. **Yilin He:** Methodology, Investigation, Formal analysis. **Kejin Wang:** Methodology, Investigation. **Wenxuan Peng:** Validation. **Side Liu:** Supervision. **Yijiang Song:** Visualization, Supervision, Funding acquisition. **Changjie Wu:** Writing – review & editing, Writing – original draft, Supervision, Funding acquisition, Data curation.

Declaration of competing interest

The authors declare that they have no known competing financial interests or personal relationships that could have appeared to influence the work reported in this paper.

Acknowledgements

The authors thank Joong Sup Shim from Faculty of Health Sciences, University of Macau, Taipa, Macau for sharing the HCT116 and RKO ARID1A isogenic cells; all the members of the Guangdong Provincial Key Laboratory of Gastroenterology for sharing materials and protocols and for the constructive discussion.

Supplementary materials

Supplementary material associated with this article can be found, in the online version, at doi:10.1016/j.neo.2024.101069.

References

[1] H. Sung, J. Ferlay, R.L. Siegel, M. Laversanne, I. Soerjomataram, A. Jemal, F. Bray, Global cancer statistics 2020: GLOBOCAN estimates of incidence and mortality worldwide for 36 cancers in 185 countries, CA Cancer J. Clin. 71 (2021) 209–249.
[2] W. Wei, H. Zeng, R. Zheng, S. Zhang, L. An, R. Chen, S. Wang, K. Sun, T. Matsuda, F. Bray, J. He, Cancer registration in China and its role in cancer prevention and control, Lancet Oncol. 21 (2020) e342–e349.
[3] G.B.D.C.C. Collaborators, Global, regional, and national burden of colorectal cancer and its risk factors, 1990-2019: a systematic analysis for the Global Burden of Disease Study 2019, Lancet Gastroenterol. Hepatol. 7 (2022) 627–647.
[4] D.I. Tsilimigras, P. Brodt, P.A. Clavien, R.J. Muschel, M.I. D'Angelica, I. Endo, R. W. Parks, M. Doyle, E. de Santibanes, T.M. Pawlik, Liver metastases, Nat. Rev. Dis. Primers. 7 (2021) 27.
[5] A. Canellas-Socias, E. Sancho, E. Batlle, Mechanisms of metastatic colorectal cancer, Nat. Rev. Gastroenterol. Hepatol. (2024).
[6] A.E. Shin, F.G. Giancotti, A.K. Rustgi, Metastatic colorectal cancer: mechanisms and emerging therapeutics, Trends. Pharmacol. Sci. 44 (2023) 222–236.
[7] E. Pretzsch, H. Niess, F. Bosch, C.B. Westphalen, S. Jacob, J. Neumann, J. Werner, V. Heinemann, M.K. Angele, Age and metastasis - How age influences metastatic spread in cancer. Colorectal cancer as a model, Cancer Epidemiol. 77 (2022) 102112.
[8] Y.H. Xie, Y.X. Chen, J.Y. Fang, Comprehensive review of targeted therapy for colorectal cancer, Signal. Transduct. Target. Ther. 5 (2020) 22.
[9] L.H. Biller, D. Schrag, Diagnosis and treatment of metastatic colorectal cancer: a review, JAMa 325 (2021) 669–685.
[10] B.G. Wilson, C.W. Roberts, SWI/SNF nucleosome remodellers and cancer, Nat. Rev. Cancer 11 (2011) 481–492.
[11] P. Mittal, C.W.M. Roberts, The SWI/SNF complex in cancer - biology, biomarkers and therapy, Nat. Rev. Clin. Oncol. 17 (2020) 435–448.

[12] B. Fontana, G. Gallerani, I. Salamon, I. Pace, R. Roncarati, M. Ferracin, ARID1A in cancer: Friend or foe? Front. Oncol. 13 (2023) 1136248.
[13] S. Jones, M. Li, D.W. Parsons, X. Zhang, J. Wesseling, P. Kristel, M.K. Schmidt, S. Markowitz, H. Yan, D. Bigner, et al., Somatic mutations in the chromatin remodeling gene ARID1A occur in several tumor types, Hum. Mutat. 33 (2012) 100–103.
[14] X.L. Wei, D.S. Wang, S.Y. Xi, W.J. Wu, D.L. Chen, Z.L. Zeng, R.Y. Wang, Y. X. Huang, Y. Jin, F. Wang, et al., Clinicopathologic and prognostic relevance of ARID1A protein loss in colorectal cancer, World J. Gastroenterol. 20 (2014) 18404–18412.
[15] W.G. Kaelin Jr., The concept of synthetic lethality in the context of anticancer therapy, Nat. Rev. Cancer 5 (2005) 689–698.
[16] A. Huang, L.A. Garraway, A. Ashworth, B. Weber, Synthetic lethality as an engine for cancer drug target discovery, Nat. Rev. Drug Discov. 19 (2020) 23–38.
[17] D.A. Chan, A.J. Giaccia, Harnessing synthetic lethal interactions in anticancer drug discovery, Nat. Rev. Drug Discov. 10 (2011) 351–364.
[18] J. Setton, M. Zinda, N. Riaz, D. Durocher, M. Zimmermann, M. Koehler, J.S. Reis-Filho, S.N. Powell, Synthetic lethality in cancer therapeutics: the next generation, Cancer Discov. 11 (2021) 1626–1635.
[19] D.G. Power, N.E. Kemeny, The role of floxuridine in metastatic liver disease, Mol. Cancer Ther. 8 (2009) 1015–1025.
[20] N. Kemeny, M. Gonen, D. Sullivan, L. Schwartz, F. Benedetti, L. Saltz, J. Stockman, Y. Fong, W. Jarnagin, J. Bertino, et al., Phase I study of hepatic arterial infusion of floxuridine and dexamethasone with systemic irinotecan for unresectable hepatic metastases from colorectal cancer, J. Clin. Oncol. 19 (2001) 2687–2695.
[21] I.J. NS, W.F. Filipe, P. Bruijn, F.E. Buisman, L.V. Doorn, P.G. Doornebosch, J. J. Holster, C. Grootscholten, D.J. Grunhagen, C.P.E. van Bommel, et al., Systemic exposure of floxuridine after hepatic arterial infusion pump chemotherapy with floxuridine in patients with resected colorectal liver metastases, Biomed. PharmacOther 162 (2023) 114625.
[22] J.A. van Laar, Y.M. Rustum, S.P. Ackland, C.J. van Groeningen, G.J. Peters, Comparison of 5-fluoro-2′-deoxyuridine with 5-fluorouracil and their role in the treatment of colorectal cancer, Eur. J. Cancer 34 (1998) 296–306.
[23] Y. Park, M.H. Chui, Y. Suryo Rahmanto, Z.C. Yu, R.A. Shamanna, M.A. Bellani, S. Gaillard, A. Ayhan, A. Viswanathan, M.M. Seidman, et al., Loss of ARID1A in tumor cells renders selective vulnerability to combined ionizing radiation and PARP inhibitor therapy, Clin. Cancer Res. 25 (2019) 5584–5594.
[24] J. Shen, Y. Peng, L. Wei, W. Zhang, L. Yang, L. Lan, P. Kapoor, Z. Ju, Q. Mo, M. Shih Ie, et al., ARID1A deficiency impairs the DNA damage checkpoint and sensitizes cells to PARP inhibitors, Cancer Discov. 5 (2015) 752–767.
[25] Z. Wang, X. Zhang, Y. Luo, Y. Song, C. Xiang, Y. He, K. Wang, Y. Yu, Z. Wang, W. Peng, et al., Therapeutic targeting of ARID1A-deficient cancer cells with RITA (Reactivating p53 and inducing tumor apoptosis, Cell Death. Dis. 15 (2024) 375.
[26] C. Sethy, C.N. Kundu, 5-Fluorouracil (5-FU) resistance and the new strategy to enhance the sensitivity against cancer: implication of DNA repair inhibition, Biomed. Pharmacother. 137 (2021) 111285.
[27] T. Sato, R.G. Vries, H.J. Snippert, M. van de Wetering, N. Barker, D.E. Stange, J. H. van Es, A. Abo, P. Kujala, P.J. Peters, H. Clevers, Single Lgr5 stem cells build crypt-villus structures in vitro without a mesenchymal niche, Nature 459 (2009) 262–265.
[28] T. Sato, D.E. Stange, M. Ferrante, R.G. Vries, J.H. Van Es, S. Van den Brink, W. J. Van Houdt, A. Pronk, J. Van Gorp, P.D. Siersema, H. Clevers, Long-term expansion of epithelial organoids from human colon, adenoma, adenocarcinoma, and Barrett's epithelium, Gastroenterology 141 (2011) 1762–1772.
[29] C. Wu, J. Lyu, E.J. Yang, Y. Liu, B. Zhang, J.S. Shim, Targeting AURKA-CDC25C axis to induce synthetic lethality in ARID1A-deficient colorectal cancer cells, Nat. Commun. 9 (2018) 3212.
[30] J. Ye, Y. Zhou, M.R. Weiser, M. Gonen, L. Zhang, T. Samdani, R. Bacares, D. DeLair, S. Ivelja, E. Vakiani, et al., Immunohistochemical detection of ARID1A in colorectal carcinoma: loss of staining is associated with sporadic microsatellite unstable tumors with medullary histology and high TNM stage, Hum. Pathol. 45 (2014) 2430–2436.
[31] R. Tokunaga, J. Xiu, R.M. Goldberg, P.A. Philip, A. Seeber, F. Battaglin, H. Arai, J. H. Lo, M. Naseem, A. Puccini, et al., The impact of ARID1A mutation on molecular characteristics in colorectal cancer, Eur. J. Cancer 140 (2020) 119–129.
[32] J.H. Park, E.J. Park, H.S. Lee, S.J. Kim, S.K. Hur, A.N. Imbalzano, J. Kwon, Mammalian SWI/SNF complexes facilitate DNA double-strand break repair by promoting gamma-H2AX induction, EMBO J. 25 (2006) 3986–3997.
[33] T. Yokogawa, W. Yano, S. Tsukioka, A. Osada, T. Wakasa, H. Ueno, T. Hoshino, K. Yamamura, A. Fujioka, M. Fukuoka, et al., dUTPase inhibition confers susceptibility to a thymidylate synthase inhibitor in DNA-repair-defective human cancer cells, Cancer Sci. 112 (2021) 422–432.